Proceedings of IMECE2005
2005 ASME International Mechanical Engineering Congress and Exposition
November 5-11, 2005, Orlando, Florida USA

IMECE2005-79295

MECHANICAL EFFECTS OF GALVANIC CORROSION OF THIN FILM POLYSILICON

David C. Miller†, Ken Gall‡, and Conrad R. Stoldt†

†Department of Mechanical Engineering
University of Colorado at Boulder
Boulder, Colorado 80309-0427

‡School of Materials Science and Engineering
Georgia Institute of Technology
Atlanta, GA 30332-0245

ABSTRACT

Mechanical, and electrical effects generated by the galvanic corrosion of polysilicon immersed in various hydrofluoric acid (HF)-based solutions are described. Micromachined test structures consisting of phosphorus-doped polysilicon in contact with a gold metallization layer are utilized. A suite of otherwise identical test (metal added) and reference (no metal) structures were used to investigate changes in key performance parameters. Corroded test structures demonstrate an increase in through-thickness strain gradient, a decrease in the characteristic frequency of mechanical resonance, no change in in-plane strain, greatly increased electrical resistance, a decrease in hardness, and a decrease in elastic modulus. Noteworthy results were observed for aqueous- hydrochloric acid, ethanol, water, ammonium fluoride (found in buffered oxide etchant), Triton-X-100, as well as vapor-HF based chemistries. This first systematic study validates preliminary experiments and demonstrates the impact of corrosion on miniaturized structures, indicating a potential influence upon the material properties, design, performance, fatigue, tribology (friction/ wear), manufacture, and packaging of micro- and nano-scale devices.

INTRODUCTION

The fabrication and assembly of micro- and nano-scale sensors and actuators relies on chemical processing steps for the realization of mechanically freestanding devices. Early studies in Micro-Electro-Mechanical Systems (MEMS) hinted at the possibility of adverse effects of such wet processing on device performance [1-3] Noted effects in these and more recent studies [4-6] include change in modulus, fracture strength, residual stress, film morphology (stress corrosion cracking and blistering), fracture morphology, surface roughness (grain boundary grooving), and fatigue life. Specifically, many of these studies examine phosphorus doped polycrystalline silicon (polySi) exposed to aqueous hydrofluoric acid (HF)-based chemistries. While the aforementioned studies suggest a significant effect, the problem of processing induced corrosion has not yet been studied systematically. Therefore we have investigated the mechanical effects of corrosion on miniaturized structures exposed to the chemistries commonly used to dissolve the silicon dioxide layers standard in surface micromachining technology.

It has been suggested that the autonomous formation of a galvanic cell may facilitate or greatly accelerate the corrosion of silicon in HF solutions [4]. Such a cell operates based on the difference in electro-chemical potential between two different materials brought into electrical contact while immersed in an electrolytic solution. In the Microsystems community, gold and polySi form one of the most common material combinations, *Figure 1*. In theory, however, even two differently doped semiconductor material layers might be sufficient, because of their intrinsically different electrochemical potential. A galvanic cell forms when an oxidizing agent, *e.g.* dissolved oxygen, is reduced at the surface of the cathode, *e.g.* the gold, *Figure 1*. The reaction motivates an anodic current, which will flow through any material electrically connected to the cathode. Electrical current may pass on as ionic current at the surface of the anode, where the transition from electrical to ionic current results in damage (oxidation) of the anode material [8] Corrosion of the anode surface may be accomplished through direct dissolution of silicon (*i.e.* porous silicon formation) or through oxidation of the entire anode surface (*i.e.* electropolishing), depending on the magnitude of the anodic current. The exact chemical reactions involved in PS formation and electropolishing are still debated, *e.g.* compare [7,9]. Similar to a galvanic cell, corrosion may be induced if an external electrical bias is applied to at least one material located in an electrolytic solution.

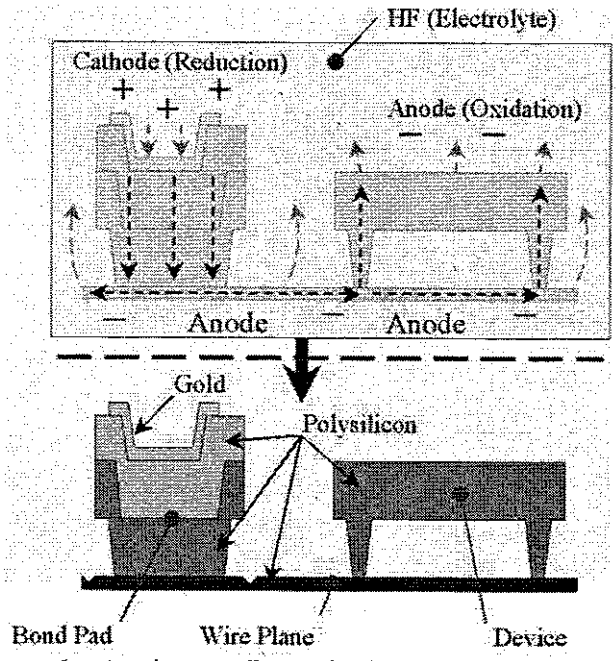

Figure 1: A galvanic cell may be formed when two different materials are immersed in an electrolytic solution, facilitating current flow (top). This anodic current results in material-dependent damage to structures in electrical contact with the cathode (bottom).

The formation of a Si-based galvanic cell has been studied in some detail, since for Si single crystals it may be used readily to manufacture porous silicon (PS) [9]. Comparison between externally biased- and autonomously corroded-polySi suggests morphological similarities [10]. Commonalties include evidenced attack along grain boundaries, dendritic PS regions, and distinct layers of damaged material. In short, morphological similarity suggests a shared root cause.

Therefore, based on the PS literature, certain aspects may be manipulated to alter the performance of a galvanic cell. First, there are methods to promote the cathodic reaction. For example, the rate of corrosion may be increased if the surface area of the metal is increased with respect to that of the silicon, if the concentration of the oxidizing agent is increased, if the circulation of the oxidizing agent is increased (through stirring), if the ambient temperature is increased, or if a more noble metal is used (according to the galvanic series for the electrolyte). Also, the presence of stronger oxidizing agents such as hydrogen peroxide (H_2O_2) or nitric acid (HNO_3) will increase the rate of corrosion, respectively. The aforementioned methods aid the cell by increasing the anodic current. The rate of corrosion can also be increased by improving the flow of ionic current at the interface between the anode and electrolyte. Lastly, many authors have noted that, especially for n-type single crystal silicon, illumination is required, and that the rate of corrosion is proportional to the extent of external illumination [9]. Illumination is thought to facilitate the cathodic reaction through the spontaneous generation of electron and hole pairs at the electrolyte interface.

For lesser anodic current, corrosion is typically limited by the cathode, for example by the supply of oxidizing agent to the metal. For greater anodic current, corrosion is typically limited at the anode, for example by the supply of fluoride ions to the silicon. As shown in the PS literature, the rate of corrosion can be increased through the use of a surfactant, such as ethanol [11], acetic acid [11], or Triton-X-100 [12]. The hydrogen-terminated surfaces typically formed on silicon immersed in HF are more hydrophobic, therefore the use of a surfactant would naturally improve the wetting of an aqueous solution. The use of a surfactant is therefore thought to facilitate corrosion by promoting the wetting of the electrolyte to the anode surface, which in turn helps remove hydrogen bubbles generated during the anodic reaction. If bubbles are prevalent at the interface, the use of a surfactant may aid corrosion, even when a lesser galvanic current is present. Note that the HF electrolytic solution serves to dissolve any native oxide that may form at the anode surface, also influencing its interfacial qualities. Removal of native oxide is not necessarily the case in galvanic alkaline solutions, such as potassium hydroxide (KOH).

In our experiments, we have observed change in performance of test structures (metal added) relative to identical, adjacently located reference structures (no metal added) Based on the literature, damage-based change in performance is attributed to anodic oxidation, i.e. autonomous formation of a galvanic cell. Therefore we systematically study the effects of such corrosion using a set of micromachined structures to monitor key performance parameters. Additionally, our experiments make use of several chemistries common to the Microsystems and PS communities.

EXPERIMENTAL

A series of designated test structures were fabricated using the Multi-User MEMS Process (MUMPS) provided by the MEMSCAP Corporation [13]. Briefly, the process can be used to create structures having one fixed and two movable layers of phosphorus-doped polySi, with material thickness in the micron range. Each polySi layer has a different material thickness and dopant concentration. In one of the final steps of the standardized fabrication procedure, a 0.5 μm thick layer of gold is adhered to the topmost polySi layer using a 20 nm thick chromium layer. All of the material layers, including the sacrificial phosphosilicate glass (PSG) interlayers are patterned using photolithographic techniques.

The "release" procedure used to free the structural layers consists of the following steps: First, the specimens are soaked in two consecutive baths of acetone for 10 minutes each in order to remove the photoresist. Next, the parts are submerged in isopropyl alcohol for 2 minutes to clean and remove any residual acetone. The parts are then soaked in deionized water (DI) for 2 minutes to remove the isopropanol. To dissolve the PSG sacrificial layers, an etch using HF-based solution is performed for separate intervals. That is, separate chips were removed from the etchant solution after different time durations, so as to characterize time dependent effect(s). The HF used in the first experiments was nominally 48% HF in water, which is hereafter

referred to as "undiluted HF" (UDHF). In addition to UDHF, HF was combined with other chemicals to investigate their influence upon the corrosion process. After immersion in HF-based solution, specimens are soaked in a (4:1) methonal:DI volumetric mixture for 10 minutes to remove and dilute any residual HF. The parts are then soaked in pure methanol for 15 minutes. Lastly, specimens are supercritically dried from the methanol solution using CO_2 to prevent surface tension induced stiction.

The light present during the chemical etching consisted of the ambient fluorescent lighting used in the cleanroom and the wet bench area, plus a 60-watt tungsten lamp, which was situated above the HF-based chemical baths. Lastly, the vapor-HF specimens were first subject to photoresist removal immediately followed by HF exposure in a chamber at MEMSCAP, Inc. The vapor-HF specimens were then subject to the entire solvent series (release procedure, acetone through methanol), however, the specimens were not re-exposed to HF.

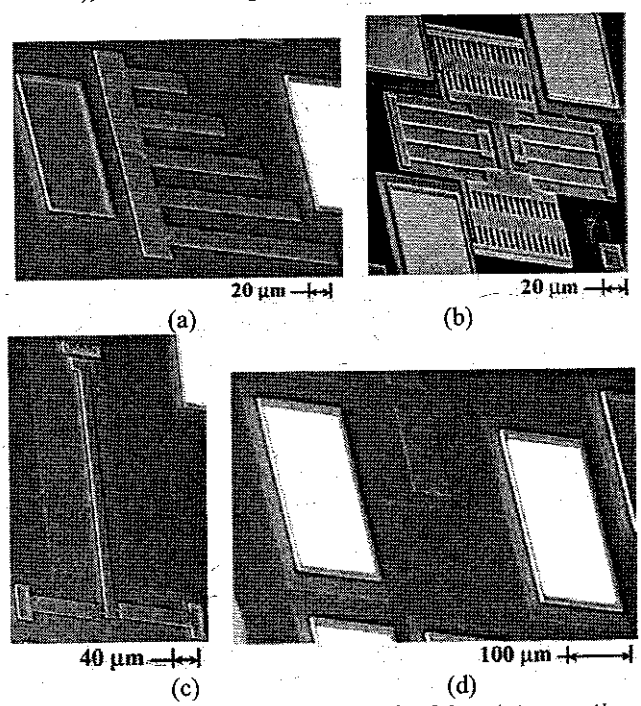

Figure 2: Test structures include (a) fixed-free (microcantilever) beams, (b) resonators (comb-drives), (c) pointers, and (d) interconnect terminated electrical traces.

The chemistries utilized include UDHF, hydrochloric acid (HCl, which may be used to eliminate trace metallic contamination in HF), ethanol (C_2H_6O), DI (H_2O, a component of buffered oxide etch (BOE)), ammonium fluoride (NH_4F, a component of BOE), Triton-X-100, and vapor phase HF (not aqueous). In addition, HCl is used by some to improve the selectivity of the SiO_2 etch for polySi with respect to that of a Si_3N_4 layer. In most cases mixtures were created on the basis of volume, however, UDHF and NH_4F were mixed on the basis of weight. Separate dice in a series were typically soaked in HF for 5 or 6 different immersion times, with 5, 10, 20, 30, 40, and 90 minutes being commonly used.

Standard test structures included cantilever beams, resonators ("comb-drives") [14], pointers [15], and electrical traces, *Figure 2*. These structures may be used to measure through-thickness train gradient (TTSG), mechanical resonant frequency, in-plane strain (IPS), and electrical resistivity, respectively. The resolution of the pointer structures used in this study was 28 με, i.e. ~ 4.5 MPa. The width of the 0.5 μm thick electrical traces was fixed at 4 μm, with the aspect ratio (AR), defined as the ratio of length to width, being 5, 50, 510, or 4800. This corresponds to a surface area ratio (SAR) of 1.17, 1.13, 0.80, and 0.21 (gold:polySi) for the traces of said geometry. That is, all traces have an equivalent area of metallization with different amounts of exposed polySi.

TTSG was characterized using a New View 200 interferometer (ZYGO Corp.), which may be used to accurately measure the curvature of beam specimens. Resonator evaluation was performed on a vacuum probe station (MMR Technologies, Inc.) at pressures ≤ 15 mTorr, thereby enhancing the quality factor (Q) of the resonance. For the experimental setup, the resonant frequency of the comb drives could be visually determined to within ±0.17 %, i.e. Q > 294. A 112545 laser (Coherent, Inc.) was used to generate a beam entering the vacuum chamber through a glass window and reflecting off of the cantilever beam specimens. By observing the shape of the laser spot, it is possible to identify the resonant frequency, since the laser spot would visually scatter at the resonant frequency. For the microcantilevers, resonant frequency could be determined to within ±0.32 %, i.e. Q > 156. Q {unitless} can be used to evaluate between ξ the damping ratio, {unitless}, k the spring constant, {N/m}, m the mass, {Kg}, c the damping coefficient, $\{N \bullet m^{-1} \bullet s^{-1}\}$, f_R the resonant frequency peak, {Hz}, f_{UL} the upper limit of resonance, {Hz}, and f_{UL} the lower limit of resonance, {Hz}, *Equation 1*. Pointers were measured using visual inspection on an optical microscope. Electrical measurements were performed using two HP 34401A multimeters to separately monitor the current and voltage supplied to an individual trace by the power supply. A Micro-Manipulator 4000 probe station was used to achieve electrical contact to the specimens. Lastly, instrumented indentation was performed on test and reference regions of polySi using a DCM machine (MTS Systems Corp.). This instrument can accurately monitor load and displacement of a Berkovitch tip into a material, and thereby continually determine material properties through the thickness according to the continuous stiffness method [16] via the Oliver-Pharr technique [17]. For reference, a <001> silicon (Si) wafer as well as a PS sample, obtained from [18], were indented, to be considered as additional reference specimens. For the polySi films, sets of (3x4) arrays of indents were made up to 20% of their thickness.

$$Q \approx \frac{1}{2\xi} \approx \frac{\sqrt{km}}{c} \approx \frac{f_R}{f_{UL} - f_{LL}} \qquad (1)$$

RESULTS

TTSG was measured first, prior to other testing; results are shown in *Table 1*. The results indicate a relative increase in curvature away from the substrate for those specimens contacted to gold. The magnitude of the effect was found to be most significant for the Poly-2, Poly-1, then Poly-1 & Poly-2 (laminate) layers, respectively. The magnitude of the effect for each of these layers was most significant when the certain HF chemistries were utilized, *Table 4*.

ELECTROLYTIC SOLUTION	CURVATURE (1/m)			
	NO METAL		METAL	
	AVG	ST DEV	AVG	ST DEV
UDHF	-66.6	6.9	-54.1	5.6
(4:1) UDHF:HCL	-71.1	3.1	-56.0	5.2
(1:1) UDHF:ETHANOL	-11.6	2.4	19.5	5.9
(1:1) UDHF:H2O	-8.9	1.7	10.6	2.4
(1:1) UDHF:NH4F	-1.3	3.8	5.5	2.8
(20:1) UDHF:TRITON	-13.5	3.7	13.8	8.8
VAPOR HF	-21.0	2.2	-19.8	3.6

Table 1: Summary of TTSG results for the Poly-2 layer.

Mechanical resonance characteristics were examined next, for both the comb-drive and microcantilever specimens. Both types of structures demonstrated a decrease in resonant frequency for those specimens connected to metal relative to those specimens not connected to metal. Furthermore, a time dependent variation was observed for most chemistries, *Figure 3*. *Figure 3* shows time dependent decrease in resonant frequency for a solution of HF and Triton. The Poly-1, Poly-2, and laminate structures (not shown) demonstrate a similar trend of decreased resonant frequency, even though the nominal f_R is quite different for each of the different material layers, *Figure 3*. Furthermore, microcantilevers of the same material layer subjected to the same HF immersion time demonstrated the same relative (percentage) decrease in resonant frequency even when the beams were of different length.

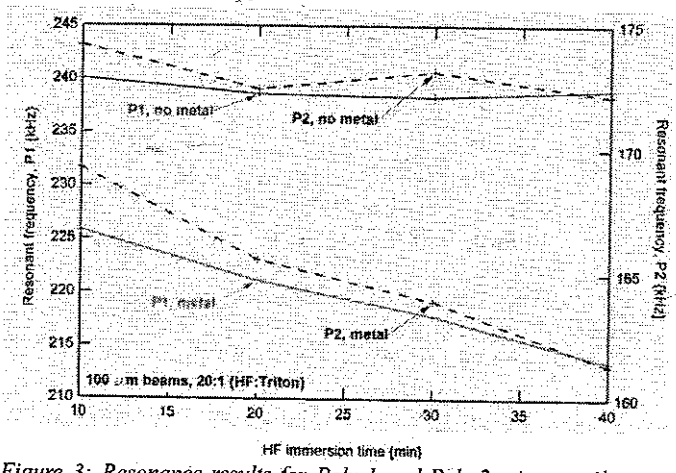

Figure 3: Resonance results for Poly-1 and Poly-2 microcantilevers immersed in a UDHF & Triton solution. Results indicate similar time dependent decrease in resonant frequency for both material layers when metal is used.

Resonance results are summarized in *Table 2* for comb-drives and in *Table 3* for microcantilevers. Similar time-dependent decrease was observed for both structure types at their f_R. The magnitude of effect was typically greater for the comb-drive specimens. The magnitude of relative decrease in f_R was greatest for the Poly-1, then Poly-2, then laminate materials layers. It is worth noting that significant decrease in f_R was observed for both the test and reference specimens soaked in a solution of HF and NH_4F. That is, NH_4F appears to attack polySi to a similar extent whether or not metal is used. On the other hand, no change in f_R was observed for parts released using vapor-HF. Lastly, there was no significant trend for change in bandwidth of resonance unique to any of the chemistries examined. Bandwidth was greatest (Q least) for the Poly-2 layer as well as for the longest microcantilevers. Bandwidth of 0.05%, i.e. Q of > 1000, was not uncommon for the shortest cantilevers or most robust comb-drives.

ELECTROLYTIC SOLUTION	% DECREASE IN RESONANT f		
	AVG	ST DEV	MAX
UDHF	4.6	2.3	6.9
(4:1) UDHF:HCL	2.6	1.6	5.3
(1:1) UDHF:ETHANOL	9.0	11.5	26.1
(1:1) UDHF:H2O	3.4	2.1	5.6
(1:1) UDHF:NH4F	11.3	19.9	41.1
(20:1) UDHF:TRITON	9.6	1.7	11.8
VAPOR HF	-0.3	0.3	-0.1

Table 2: Summary of mechanical resonance results for Poly-1 comb-drives (see Figure 2 (b)).

ELECTROLYTIC SOLUTION	% DECREASE IN RESONANT f		
	AVG	ST DEV	MAX
UDHF	1.3	0.8	2.2
(4:1) UDHF:HCL	0.7	0.4	1.5
(1:1) UDHF:ETHANOL	9.2	4.1	13.5
(1:1) UDHF:H2O	5.2	2.9	8.4
(1:1) UDHF:NH4F	6.4	N/A	6.4
(20:1) UDHF:TRITON	8.3	2.1	11.0
VAPOR HF	0.0	0.0	0.0

Table 3: Summary of mechanical resonance results for banks of Poly-1 microcantilevers (see Figure 2 (a)).

Examination of IPS did *not* demonstrate significant difference between the test and reference specimens within the resolution of optical microscopy. Measurements of –51.1, -91.9, and –22.8 µε were obtained for the Poly-1, Poly-2 and laminate layers respectively. Assuming a material modulus of 163 GPa, this corresponds to the compressive stress of 8.2, 14.7, and 3.6 MPa for the respective layers. The measured strain and stress values are roughly as would be expected for each of the material layers, which are measured during every fabrication run [13].

Unlike the IPS, electrical resistance was significantly affected upon exposure to HF. For the trace test structure, all specimens were metallized, but reference measurements could be obtained from dice never exposed to HF. In general, a very significant, time-dependent (several orders of magnitude) increase in electrical resistance could be observed as a consequence of HF immersion, *Figure 4*. *Figure 4* shows the increase in resistance for traces immersed in UDHF relative to the specimen never immersed in HF. In all cases (except for

vapor-HF) traces exposed to the HF-based chemistries for maximum immersion time of 90 minutes became nonconductive, *i.e.* resistance greater than the 10 MOhm input impedance of the test equipment. For many of the chemistries examined, traces became nonconductive when immersed in HF for 20, 30, or 40 minutes. In general those traces with the least AR, *i.e.* greatest SAR, were most readily affected. For example, the AR 4800 traces were the last to become nonconductive and only for the greatest HF immersion times. Note that the 5 and 50 AR traces have a very similar SAR. Additionally, the specimens exposed to a mixture of HF and NH_4F were greatly affected by the solution, with minimal data available after 10 minutes exposure. Further information concerning *Figure 4* as well as *Figure 1* may be found in [19].

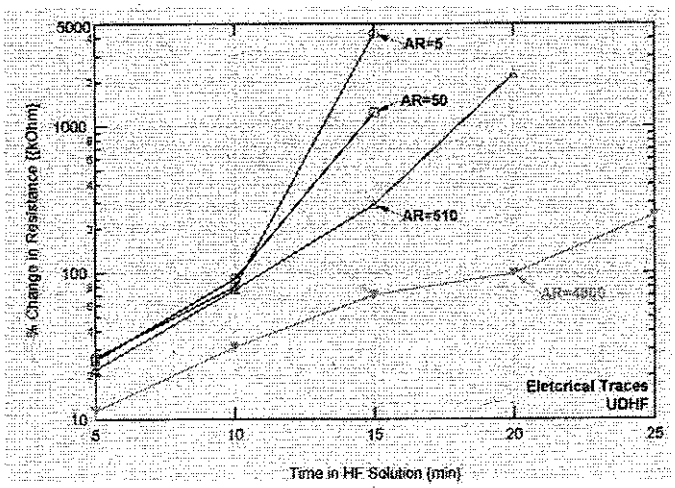

Figure 4: Summary of I/V results for Poly-0 traces of different AR soaked in UDHF for immersion times of 5, 10, 15, 20, and 25 minutes.

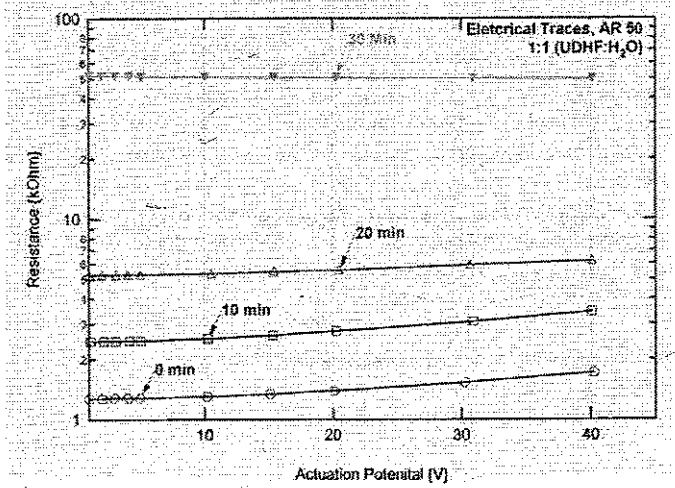

Figure 5: I/V results for AR 50 traces soaked in a UDHF & DI mixture for immersion times of 0, 10, 20, and 30 minutes.

Figure 5 shows the time dependent nature of the increase in resistance resulting from exposure to HF. In this case, the solution examined consisted of a mixture of HF and DI. For those parts immersed for 0, 10, or 20 minutes, electrical resistance is seen to increase in a logarithmic manner. The additional AR 50 specimens immersed in the solution for 40 and 90 minutes were found to be nonconductive. The resistance of the 0, 10, and 20-minute traces in *Figure 5* could be described as ohmic (voltage-independent) in nature, with some slight variation according to actuation potential.

Results of indentation testing for the Poly-0 layer are shown in *Figure 6* and *Figure 7*. The figures show several test specimens compared to a Si (<001> oriented) wafer as well as a PS specimen. In most cases, the test specimens have been exposed to HF for the period of 90 minutes so as to render obvious results. So far, indentation of test specimens exposed to HF for lesser duration times show similar results, but lesser in magnitude of effect. Except for the HF and NH_4F mixture, reference specimens of Poly-0 also exposed to the various HF chemistries show little or no change, *i.e.* they are similar to the <001> Si or vapor-HF test specimens. *Figure 6* and *Figure 7* demonstrate a very significant decrease in hardness and modulus for test specimens exposed to several of the HF chemistries examined. Decrease in hardness and modulus was also observed for Poly-1 test specimens subjected to the same HF chemistries as in the figures. The magnitude of effect was generally not as significant as the Poly-0 material, with data ranging in between the <001> Si and PS reference specimens. Other measurable indentation parameters, such as P/h (load/displacement), relative amount of retained energy, sink-in ratio, P/S^2 (tip area independent parameter [17]), and K (elasticity and plasticity decomposition parameter [17]) were greatly altered by some of HF chemistries examined. Lastly, it is worth noting that the hysteresis behavior typically observed in the P/h curve and thought to be associated with phase transformation of Si [20] was not always observed in the Poly-0 test specimens exposed to HF plus C_2H_6O, NH_4F, or Triton solutions. Hysteresis between the first unloading and second loading profiles was not always observed in the indentation profiles for the PS reference sample either.

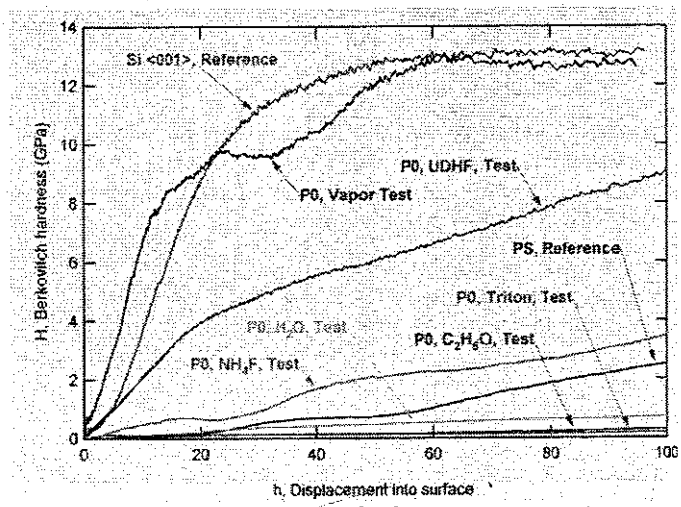

Figure 6: Indentation hardness results for various test specimens as well as single crystal <001> Si and PS reference specimens.

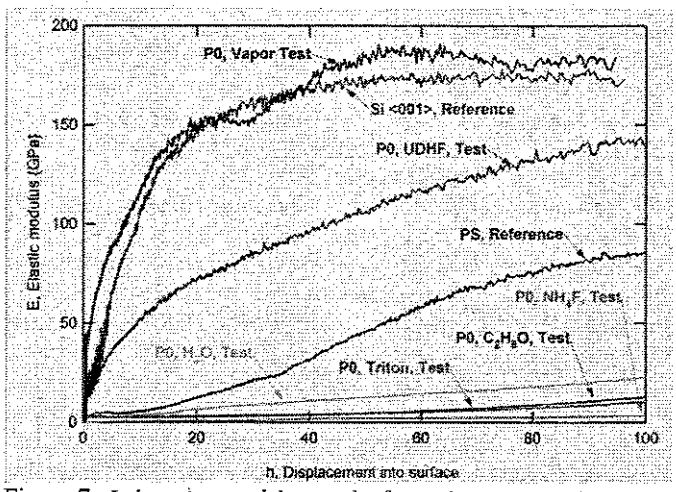

Figure 7: *Indentation modulus results for various test specimens as well as single crystal <001> Si and PS reference specimens.*

Results of the various experiments and chemistries are summarized in *Table 4*. In general, no significant change in IPS was observed for any of the chemistries examined. Effect upon TTSG, mechanical resonance, electrical resistance, modulus, and hardness was found to range from minimal (least) to significant (maximum), for the various chemistries examined. Intermediate change in performance is labeled as "moderate" in *Table 4*. Sub-minimal (threshold of measurement) difference was observed for parts etched using vapor-HF. For many of the measured parameters UDHF as well as HCl solutions generated similar results. Solutions mixed with C_2H_6O, H_2O, NH_4F, and Triton often shared similar results and collectively will be referred to as the "high impact" chemistries.

Etchant	Change in TTSG	Change in IPS	Change in mechanical resonance	Change in electrical resistance	Change in hardness & modulus
Undiluted (48%) HF	Moderate	None	Minimal	Significant	Moderate
4:1 (UDHF:HCl)	Moderate	None	Moderate	Minimal	Minimal
1:1 (UDHF:Ethanol)	Significant	None	Significant	Minimal	Significant
1:1 (UDHF:H2O)	Significant	None	Moderate	Moderate	Significant
1:1 (UDHF:NH4F)	Minimal	None	Significant	Significant	Significant
20:1 (UDHF:TRITON)	Significant	None	Significant	Moderate	Significant
VAPOR HF	None	None	None	None	None

Table 4: Summary of mechanical results for various HF-based chemistries examined.

DISCUSSION

TTSG results indicate a real and measurable change in curvature for the microcantilevers. These results, obtained from samples made in the MUMPS 61, 63, and 64 fabrication runs, are similar to preliminary results obtained from the MUMPS 58 fabrication run [22]. The new results are different from those for the otherwise identical first generation devices in that curvature, in some cases, increased above the neutral (zero curvature) position, *Table 1*, and did not just become less negative (flatter) in magnitude [22]. The curvature is therefore not necessarily decreasing towards a neutral state as was previously speculated. Like many of the other results, *Table 4*, change is TTSG was greatest for the high impact chemistries, specifically C_2H_6O, H_2O, and Triton. TTSG may have been affected in the other high impact chemistry, NH_4F, and is not as noticeable since the test and reference specimens may have been both corroded to a similar extent.

At this point it is unclear what operant mechanism may motivate the change in TTSG. Change in curvature may come about as a result of stress corrosion, i.e. preferential attack on strained material. For unmetallized reference specimens, the Poly-2 layer typically has the greatest curvature, followed by the Poly-1, and then laminate layers, respectively. Therefore HF may preferentially attack the Poly-2 layer, since it would have the greatest intrinsic strain energy, as motivated by its greater curvature. Change in curvature may also come about due to through-thickness variation in morphology in the polySi layers. For example there may be a variation in grain density or grain geometry that would make either the top or bottom surface more resistant to corrosion. More specifically, if there were many through-thickness tapered grains, HF may attack the free surface with the larger number of smaller grains, since attack would be favored at high-energy grain boundaries. It is worth noting that during fabrication, the Poly-2 layer is subject to relatively lower temperature anneals. Therefore the material has had the least opportunity for its grain morphology or material density to stabilize, which might make it more prone to attack. Alternately, difference in TTSG results may come about for other reasons, such as the different exposed SAR for the polySi layers (they are of different thickness). Change in curvature may also be magnified or attenuated by the stiffness of the layers (which depends upon the cube of their thickness).

Curvature, K $\{m^{-1}\}$, may be related to the deflection of the beam's free-end, δ {m}, if its length is known, L {m}, *Equation 2*. In most cases, the beam's length is much greater than the displacement of its tip and a reasonable approximation is obtained if the δ^2 term in the denominator is neglected. Curvature of a monolithic beam may also be related to the deformation through solid mechanics if the moment, M {N•m}, material's elastic modulus, E {Pa}, and second moment, I $\{m^4\}$ are known, *Equation 2*. Lastly, the TTSG (curvature) may be related to the local strain, e {ppm}, if the distance from the geometric midplane (in the through-thickness direction) is known, z {m}. Depending on the physical circumstance, within the elastic regime, local strain may be related to local stress when multiplied by the material modulus or biaxial modulus.

$$K = \frac{2\delta}{\delta^2 + L^2} = \frac{M}{EI} \qquad (2)$$

$$e = Kz \qquad (3)$$

It is worth noting that similar to [22], some variation in TTSG was observed for microcantilevers of different length. For example, the longer Poly-2 beams typically also had the greatest (most positive) curvature. The opposite and same trends were true for the Poly-1 and laminate layers, respectively. It is not clear if this behavior originates as an artifact of proximity of the beam's anchor or for some other reason.

No significant change in IPS was observed for any of the specimens exposed to HF. This indicates that there is no great change in strain in the material's in-plane direction. Attack on the material may occur uniformly in this direction and/ or in a manner that does result in a net change in IPS. Change in intrinsic (in-plane) residual stress was, however, observed in [2]. It is worth noting that the stress in the test specimens exposed to HF is subject to some change based on change in TTSG, *Equation 3*. Such change in stress might manifest itself more readily in membranes or even more complicated structures. At this point, however, there does not seem to be a significant motivation for the stress to change that is solely dependent upon the in-plane direction.

Mathematical analysis of the resonance results provides some physical insight into the corrosion phenomenon. Change in f_R may be represented using *Equation 4*. *Equation 4* may be used to relate between the quantities of resonant frequency, f_R {Hz}, effective spring constant, k {N/m}, mass, m {Kg}, elastic modulus, E {Pa}, second moment, I {m^4}, beam length, L {m}, material density, ρ {Kg/ m^3}, beam width, b {m}, beam thickness, t {m}, and the mathematical constant, π. The middle and right-most expressions in *Equation 4* are valid for a cantilever beam. The equation, while general in nature, is useful since it suggests that in order for the resonant frequency to decrease the quantities k, E, or t must decrease relative to the quantities m, ρ, or L. From a practical mechanics standpoint, *Equation 4* suggests that all metallized resonators' spring constant (stiffness) must decrease, since corrosion is unlikely to result in added mass. From a practical materials standpoint, *Equation 4* suggests that the test microcantilevers' elastic modulus and/or thickness must decrease, and in a manner more significant than any decrease in density or beam length. A decrease in modulus was observed in the indentation experiments, lending validity to the model. Similarly, a decrease in thickness was observed for at least some chemistries [22], as might also be predicted by *Equation 4*. Lastly, the observed decrease in f_R, *Table 2* and *Table 3*, is significant. As a benchmark for comparison, the use of design geometry to alter f_R was found to effect unmetallized MUMPS fabricated microcantilevers by as much as 1.8% [21].

$$f_R \approx \frac{1}{2\pi}\sqrt{\frac{k}{m}} = \frac{1}{2\pi}\sqrt{\frac{3EI}{L^3}\frac{1}{\rho bLt}} = \frac{1}{4\pi}\sqrt{\frac{Et^2}{\rho L^4}} \qquad (4)$$

Similar relative magnitude of change seen for microcantilevers within the same test array may have important implications. Change in f_R was observed to occur in a time dependent and uniform manner for each pair of test and reference arrays examined. That is to say, a low pass filter (RC-time delay) effect for the Poly-0 interconnect wiring is not suspected. If the decrease in f_R were motivated by a change in the resistance of the Poly-0 (or other) wiring, than the relative decrease in f_R would be different for each beam within an array as would be motivated by the vastly different f_R of beams of different length, *Equation 4*. Instead the f_R of the beams within the same test array decreased by the same relative (percentage) amount. Furthermore, none of the beams exhibited an aberrant change in f_R. This may suggest that, for a large enough volume of polySi material, the attack on each of the layers occurs in a consistent manner.

The resonance results for the comb-drive and microcantilever specimens compare favorably. Change in f_R was of similar magnitude, being greater for the comb-drive specimens, *Table 2* and *Table 3*. For both test structures, the greatest and least change in f_R occurred for the same material layers. This and the fact that the observed relative decreases in f_R were of the same order of magnitude lend validity to the measurements.

The different extent of damage to the different polySi layers is most likely associated with the unique dopant concentration inherent to each of the layers. Dopant concentration (as well as visual discoloration of test specimens [22]) decreases between the Poly-0, Poly-1, Poly-2, and laminate layers, in that respective order. Based on the resonance results, damage to the structural layers decreased between the Poly-1, Poly-2, and laminate layers, respectively. Note that the thickness of the layers decreases between the laminate, Poly-1, and Poly-2 layers, respectively, i.e. not the same order corresponding to magnitude of decrease in f_R. Therefore, the proclivity for damage does not most immediately correspond to the thickness, *i.e.* material volume, surface area or mechanical stiffness. Instead change is though to be related to dopant concentration. The morphology of PS is known to depend upon dopant concentration, in particular for highly doped n-type silicon [9]. Furthermore, because the dopant concentration is known to affect the morphology of polySi, it may likewise influence the damage mechanisms for material subject to corrosion. For example, the number of grain boundaries or grain boundary porosity might aid the HF.

The magnitude of decrease in f_R was usually slightly greater for the comb-drives than the microcantilevers. This may be related to the different geometry of these structures. Even though both structure types have the same thickness, HF may be able to further permeate into flexures of the comb-drives because of their smaller cross-section size (they are 3 μm wide) as opposed to the beam shafts, which are 20 μm wide. Furthermore, flexures made using a different design geometry or fabrication processes, may have a cross section ≤ 1 x 1 μm^2 making them more prone to damage than the structures used in this study. Vulnerability could be enhanced because the material may be more thoroughly permeated from all of its free surfaces. That is, the path of damage (whether based on grain boundaries, diffusion, etc.) is lesser for smaller geometries.

Electrical characterization indicates very significant change in performance occurs as the result of exposure to HF. Results in this more extensive study (much greater sample size) differ from those in preliminary experiments [22] in that no extreme non-linear behavior is observed. The previous work indicated non-ohmic behavior, particularly at lesser actuation potentials. Difference between the experimental results is attributed to the better equipment used in the more recent experiments, *Figure 4*

and Figure 5, which is more capable of accurately monitoring the smaller electrical currents generated at the low voltage.

While measurements were made using a two-probe method, not the highly sensitive four-point probe technique, the electrical characterization is still expected to be quite accurate. Foremost, resistance measurements are made using I/V profiles, *i.e.* direct measurement of electrical current and voltage. Furthermore, electrical contact to the trace test structures is established by contacting probes directly to gold metallization, which should minimize the contact resistance of interconnectivity. Gold, used on all of the trace specimens, is a material known for its minimal contact resistance of interconnectivity. System, including probe to probe, resistance was 4.9± 1.0 Ohms when both probes were contacted to the gold on the same wire bond pad. Additionally, the resistance of the auxiliary electrical connection from bond pad through the substrate to another bond pad was probed to be 44±5 Ohms for *all* the specimens exposed to the various HF-based solutions for 90 minutes. That is, the contact resistance of connectivity between layers is an order of magnitude lesser than that of the specimen of least nominal resistance, i.e. 150 Ohm. The electrical results thus represent a real phenomenon, with the observed increase in resistance being several orders of magnitude greater than the observed nominal contact resistances.

Note that for those specimens exposed to a HF and HCl mixture for an extended period of time, some delamination was observed at the periphery of the Metal layer. Delamination, including complete removal of gold from polySi, has been observed for MUMPS fabricated parts immersed and actuated (constant current) in a saline (H_2O and sodium chloride) solution for an extended period of time [21]. Delamination is therefore may be associated with the Cl^- ion, which may catalyze or directly attack the chromium adhesive layer. In this study, delamination was not extensive, being limited to within a 10 – 20 μm periphery around the edges of metallized features; therefore it is not expected to greatly affect the results.

Slight non-linearity was observed in the resistance measurements, *Figure 5* Non-linearity at higher voltages is attributed to the Joule heating thought to be associated with scattering of the majority (n-type) electron carriers at grain boundaries. Joule heating is thought to be most prevalent in the specimens immersed in HF for 0 and 10 minutes, *Figure 5*. In contrast, resistance is actually seen to decrease as voltage is increased for the 30-minute specimen, *Figure 5*. Similar behavior was observed in a few of the other chemistries examined, in particular at those immersion times just prior to nonconductivity. It is unclear if this behavior is associated with the damage mechanism affecting resistance, so-called "second breakdown" of the material, or another phenomenon.

What is the cause of the increase in electrical resistance? Added resistance might be explained if the corrosion process results in the leaching of phosphorus dopant, rather than the sole consumption of polySi. If dopant were depleted, the material would lose conductivity, approaching a more natural intrinsic semiconductor behavior. Alternately, the results may also be explained if the nature of the physical damage is similar to the results seen in porous polySi studies [10]. In this study, the polySi is attacked along the grain boundaries. If corrosion is sufficiently extensive, grain boundaries might become completely severed, decreasing the effective volume of material available as a path for electrical conduction. Given sufficient exposure time, this mechanism would effectively sever a trace at one or more locations along its length. Lastly, for some of the chemistries, there may be an outright consumption of material. Volumetric loss would lead to an increase in resistance, since electrical resistance is known to depend upon the geometry of the trace/ lead.

In addition to these possible explanations, the attack on the polySi exposed to UDHF is likely to be extensive, but extremely localized. The attack may be localized due to the build-up of hydrogen bubbles on the anode surface as a consequence of the active chemistry. In this case, a small portion of the trace is still in contact with the HF and the density of the corrosion current transmitted at the active interface is greatly magnified resulting in very significant localized corrosion. If so, a relatively narrow trace will eventually sever at one or more locations along its length, resulting in an open circuit and the cession of the galvanic corrosion process.

The resonance results, like the electrical resistance results, exhibit a distinct dependence upon immersion time, *Figure 3*, and *Figure 4*. Time dependence might be logically expected as more corrosion may occur as long as the test specimen is maintained in HF. Curiously, the decrease in f_R tends to vary linearly according to time, whereas the increase in resistance tends to vary logarithmically with time. Difference in the time dependence reflects the difference that the structural changes have on the operant mechanisms controlling the measurements.

While the indentation studies do not sample a large volume of material, they provide powerful insight. Assuming an average grain diameter of 350 nm, based on the previous work of the authors [4] as well as an ideal Berkovitch geometry, the surface of the tip is expected to be in contact with approximately 1, 2, and 10 grains at the indentation depths of 50, 100, and 200 nm, respectively. While the indentation results do indicate some very significant change in material properties, the measurements truly apply to the free surface of the polySi layers examined. In particular, several of the high impact chemistries indicate a major decrease in hardness, being similar to the PS reference sample. Some of the specimens exposed to these same high yield chemistries, as well as the PS reference specimen, were not seen to exhibit the P/h hysteresis behavior typical of phase-transforming Si. Loss of phase activity might be possible, even if PS had formed only at the free surface of the polySi, because Si is a chemically instable material. In fact, PS is known to readily oxidize in an ambient environment, unless it is surface functionalized [18]. Perhaps as opposed to a change in chemistry, phase transformation might also be forgone if the material morphology was affected such that the indentation region did not achieve sufficient pressure in order to change phase. For other samples, however, decrease in hardness is not nearly as significant. In these cases, the results may indicate the presence of a thick oxide layer, as typically formed during electropolishing. Alternately these results may simply indicate a

normal native oxide, which for silicon is typically 2-4 nm thick [4].

Increase in electrical resistance caused by galvanic corrosion is very likely to effect thermally actuated devices. The relatively large electrical current required to drive a device that is volumetrically small limits the magnitude of the actuation potential to a correspondingly small value. Our work indicates that this would render common thermally actuated devices nonfunctional if they are prepared in pure HF. Indeed, for devices subjected to sufficient corrosion, change in the characteristic actuation curve was evident. Further, we have seen thermal actuators [23,24] (as well as electrostatic comb-drives [14] and microcantilevers) rendered nonfunctional, *i.e.* immobile, because of galvanic corrosion. For these completely failed devices, as well as some of the test structures in this study, it is unclear exactly when the damage to the devices ceased. After all, anodic current could be terminated if the traces become highly- or non-conductive. As seen in failed thermal actuators, use of Poly-0 is not required to render nonconductive devices. For the MUMPS polySi layers, however, the Poly-0 may be preferentially sacrificed because of its higher dopant concentration.

Given the risk of damage caused by galvanic corrosion, what steps may be taken to limit its extent or prevent it outright? As described in the introduction, use of design considerations, such as minimal SAR for metal and polySi, as well as processing considerations, such as minimal exposure time to HF, are generally helpful in reducing damage to metallized specimens. Note that some of the chemicals typically used as surfactants for PS manufacture, *i.e.* C_2H_6O and Triton, are regarded as high impact chemistries in this study. At this point, it is unclear whether these surfactants are better or worse than the other chemistries examined, but post-test morphological investigation of specimens is currently underway. As most of its test specimens where minimally affected, use of vapor-HF may be an outright solution. Vapor-HF may be a viable solution provided it does not cause other problems, such as particulate contamination, [1]. Use of vapor-HF may eliminate the electrolytic nature (ionic current) of the chemical cell, thereby preventing flow of the damaging anodic current. Note that the vapor-HF specimens demonstrate that the corrosion damage is unique to HF, since these parts were later exposed to all of the other post-processing solvents. Use of structural materials other than polySi or Si might be another possible solution, because of greater chemical inertness or lesser galvanic potential.

On the other hand, NH_4F, a component of BOE, caused corrosion for both test and reference samples. Water, another component of BOE also at times caused significant corrosion. This suggests that, at least for polySi, BOE may not be harmless. For example, brief immersion in BOE is often used on wafers prior to subsequent material deposition, in order to remove native- or surface-oxides. BOE have greater effect on polySi as opposed to single crystal Si, because of its higher intrinsic energy, i.e. greater number of grain boundaries.

While the effects of corrosion are evident in micro-scale devices, the effects will be even more significant for nano-scale devices. At the nano-scale, the effects of surface-driven phenomenon such as diffusion, chemical-reaction, and corrosion are in general greatly enhanced. Also for a device fabricated to nanometer tolerances, there is less material present magnifying the effects of material loss. Furthermore, the surface area to volume ratio for a nano-scale structure will additionally favor any metallization used in electrical interconnects. Therefore, the use of relatively long electrical traces and lengthy etch times as in our experiments may in fact sometimes under-represent the effects of corrosion on a nano-scale device. Note also for some miniature scale applications there may be instances where the use of so-called "etch release holes" to minimize exposure time to HF cannot be used and prolonged exposure to HF is required. In other cases post-processing techniques, such as flip-chip bonding, may require lengthy immersion in HF.

Galvanic corrosion may pose very serious problems that must be taken into account when determining material properties. Historically, researchers have tried to ascertain a single value for the material modulus, and Poisson's ratio of a polySi material fabricated using specific equipment according to specific settings. If galvanic corrosion is found to affect the polySi material itself, then this approach may have to be reconsidered. In this case, the post-processing of the material would hold influence upon the material properties. No single set of material property values would apply, since it is be dependent upon the post-processing procedure used. The post-processing procedure (specifically the chemical etching release process) would have to be identified for proper discussion of material properties.

Note that in the literature, a wide range of material properties for polySi is not uncommon, even for round-robin studies of structures made using the same fabrication batch. Corrosion of a monolithic polySi structure has been observed as a consequence of exposure to HF, resulting in a change of the morphology of the material [4]. Because galvanic corrosion during etching in HF also affects material properties, *e.g.* as seen in indentation, then the reported variance in measured material properties is logically inevitable. Some of the property values offered in the literature might represent an ideal upper bound, whereas others are diminished as the result of galvanic corrosion.

CONCLUSIONS

We have demonstrated the corrosion of phosphorus-doped polySi when contacted to a gold metallization layer and exposed to commonly used HF chemistries, *i.e.* standard post-processing procedures. A suite of otherwise identical test (metal added) and reference (no metal) structures revealed change in key performance parameters. Noteworthy results were observed for the various aqueous- HCl, C_2H_6O, H_2O, NH_4F, Triton, as well as vapor-HF-based solutions. Test structures demonstrate an increase in TTSG, a decrease in the frequency of mechanical resonance, no change in IPS, greatly increased electrical resistance, a decrease in indentation hardness, and a decrease in mechanical modulus relative to reference structures.

Change in TTSG may be responsible for the change in residual stress observed past HF-based immersion studies. The extent of damage observed in our experiments suggests that, between otherwise identical test structures, material dopant concentration as well as HF immersion time are dominant parameters affecting the extent of damage. At this point, it is unclear whether the damage to the polySi layers occurs through porous silicon generation or electropolishing for any of the various chemistries examined. The effects of galvanic corrosion will readily influence thermally actuated devices, since their operation is critically dependent upon drive current. Vapor-HF may be an advantageous post-processing technology, since it was seen to circumvent galvanic damage. Oppositely, NH_4F, a principle component of BOE, caused corrosion for both test and reference samples, suggesting that BOE is not a benevolent mixture. The effects of galvanic corrosion on nano-scale devices is expected to be very significant, since these devices are so sensitive to surface driven phenomenon and do not contain a significant amount of structural material. Corrosion, which has largely gone previously unnoticed, may explain the variability in material properties seen in the literature. Because corrosion affects the mechanical performance, the post-processing procedure may have to always be considered, in addition to the polySi deposition procedure, regarding material properties. This first systematic study validates preliminary experiments and demonstrates the impact of corrosion on miniaturized structures, indicating a potential influence upon the material properties, design, performance, fatigue, tribology (friction/ wear), manufacture, and packaging of micro- and nano- scale devices. This suggests the need for greater understanding of the corrosion process as well as consideration of its consequences.

ACKNOWLEDGEMENTS

The authors acknowledge support from the University of Colorado at Boulder for this work.

REFERENCES

1. T.A Lober and R.T. Howe, 1990, "Surface Micromaching Processes for Electrostatic Microactuator Fabrication", Proc. IEEE MEMS, pp. 59-62.
2. J.A. Walker, K.J. Gabriel and M. Mehregany, 1990, "Mechanical Integrity of Polysilicon Films Exposed to Hydroflouric Acid Solutions", Proc. IEEE MEMS, pp. 56-60.
3. D.J. Monk, P.A. Krulevitch, R.T. Howe and G.C. Johnson, 1993, "Stress-Corrosion Cracking and Blistering of Thin Polycrystalline Silicon Films in Hydroflouric Acid", Proc. Mat. Res. Soc. Symp., 308, pp. 641-646.
4. I. Chasiotis and W.G. Knauss, 2001, "The Mechanical Strength of Polysilicon Films: Part 1. The Influence of Fabrication Governed Surface Conditions", J. Mech Phys. Solids, 51, pp. 1533-1550.
5. H. Kahn, C. Deeb, I Chasiotis and A.H. Heuer, 2005, "Anodic Oxidation During MEMS Processing of Silicon and Polysilicon: Native Oxides Can be Thicker Than You Think", J MEMS, *in review.*
6. O.N. Pierron, D.D. Macdonald, and C.L. Muhlstein, 2005, "Galvanic Effects in Si-Based Microelectromechanical Systems: Thick Oxide Formation and its Implications for Fatigue Reliability", Appl. Phys. Lett., 78 (21), pp. 211919-211921.
7. X. Xia, C. Ashruf, P. French and J. Kelly, 2000, "Galvanic Cell Formation in Silicon/ Metal Contacts: The Effect on Silicon Surface Morphology", Chem. Mater. 12, pp. 1671-1678.
8. O. Bisi, S. Ossicini and L. Pavesi, 2000, "Porous Silicon: a Quantum Sponge Structure for Sdilicon Based Optoelectronics", Surf. Sci. Rep., 38, pp. 1-126.
9. X.G. Zhang, S.D. Collins and R.L. Smith, 1989, "Porous Silicon Formation and Electropolishing of Silicon by Anodic Polarization in HF Solution", J Electrochem. Soc., 136 (5), pp. 1561-1565.
10. P. Guyander, P. Joubert, M. Guendouz, C. Beau, and M. Sarrett, 1994, "Effect of Grain Boundaries on the Formation of Luminescent Porous Silicon from Polycrystalline Silicon Films", Appl. Phys. Let, 65 (14), pp. 1787-1789.
11. G. Sotgiu, L. Schirone, and F. Rallo, 1997, "On the Use of Surfactants in the Electrochemical Preparation of Porous Silicon", Thin Solid Films, 297, pp. 18-21.
12. J. Das, S.M. Hossain, S. Chakraborty and H. Saha, 2001, "Role of Parasitics in Humidity Sesning by Porus Silicon", Sens Act A, 94, pp. 44-52.
13. D. Koester, A. Cowen, R. Mahadevan, M. Stonefeild, B. Hardy, 2003, Poly-MUMPs Design Rules: Revision 10, MEMSCAP Inc.
14. W.C. Tang, T.C.H. Nguyen and R. Howe, 1989, "Laterally Driven Polysilicon Resonant Microstructures", Sens. Act A, 20, pp. 25-32.
15. B. P. van Drieenhuizen, J.F.L. Goosen, P.J. French, and R.F. Wolffenbuttel, 1993, "Comparison of Techniques for Measuring Both Compressive and Tensile Stress in Films, Sens. Act. A, 37-38, pp. 756-765.
16. D.L. Joslin and W.C. Oliver, 1990, "A new method for analyzing data from continuous depth-sensing microindentation tests", J. Mater. Res., 5, pp. 123-126.
17. W.C. Oliver and G.M. Pharr, 2004, "Measurement of hardness and elastic modulus by instrumented indentation: Advances in understanding and refinements to methodology", J. Mater. Res., 19, pp. 3-20.
18. Z. Shen, J.J. Thomas, C. Averbuj, K.M. Broo, M. Englehard, J.E. Crowell, M.G. Finn, and G. Siuzdak, 2001, "Porous Silicon as a Versatile Platform for Laser Desorption/ Ionization Mass Spectrometry", Anal. Chem., 73 (3), pp. 612-619.
19. D.C. Miller, K. Gall, and C.R. Stoldt, 2005, "Galvanic Corrosion of Thin Film Polysilicon: Morphological, Electrical and Mechanical Effects", Electrochemical and Solid-State Letters, 8, pp. G223-G226.
20. V. Domnich, D. Ge, and Y. Gogotsi, 2004, "Indentation-Induced Phase Transformations in Semiconductors", in High-Pressure Surface Science and Engineering, IOP: Philadelphia.
21. A.B. Hartman, F.W. DelRio, and D.C. Miller, or H.V. Panchawagh, 2005, University of Colorado, Unpublished research.
22. D.C. Miller, K. Gall, and C.R. Stoldt, 2004, "Galvanic Cell Formation during MEMS Release Processes: Implications for Sub-micron Device Fabrication". Proc. ASME Inter. Mech. Eng. Cong. & Exp., 62088, pp. 1-10.
23. R. Cragun and L.L. Howell, 1999, "Linear Thermomechanical Microactuators", Proc. ASME IMECE, pp. 181-188.
24. J.R. Reid, V.M. Bright and J.H. Comtois, 1996, "Arrays of Thermal Micro-Actuators Coupled to Micro-Optical Components", Proc. SPIE, 2865, pp. 74-82.